9.19 Microscale PIV Wind Tunnel Investigations

Contributed by:
M. Raffel, C. Rondot, D. Favier, K. Kindler

Detailed studies of the boundary layer profile and the characteristics of the flow velocity distribution close to the leading edge of a helicopter blade profile were conducted using 2C-PIV. The relatively small scales of flow structures related to dynamic stall, the study in which the flow field has been measured with a relatively high spatial resolution. The feasibility of μ-PIV measurements utilizing a mirror telescope in a wind tunnel has been demonstrated successfully. The spatial resolution of approximately 50 μm allowed for an assessment of the different turbulence models and damping coefficients for the improvement of CFD predictions.

Table 9.23. PIV recording parameters for microscale wind tunnel investigations.

Flow geometry	Boundary layer on an OA209 blade tip model
Maximum in-plane velocity	$U_{\max} = 10\,\mathrm{mm/s}$
Field of view	$1.658 \times 1.358\,\mathrm{mm}^2$
Interrogation volume	96×96 pixel
Observation distance	$z_0 = 35.5\,\mathrm{cm}$
Recording method	double frame/single exposure
Recording medium	CCD camera, 1280×1024 pixel
Recording lens	Mirror objective lens, $M = 4.86$, $f_{\#} = 6$
Illumination	Nd:YAG laser[a] $2 \times 200\,\mathrm{mJ/pulse}$
Pulse delay	$\Delta t = 10\,\mathrm{ms}$
Seeding material	oil droplets ($d_\mathrm{p} \simeq 1\,\mu\mathrm{m}$)

[a] frequency doubled

9.19.1 Introduction

Over the past decade, considerable progress has been made in the development of performance prediction capabilities for isolated helicopter components. Modern CFD methods deliver promising results for moderate operation conditions. The prediction of high-speed and high-load cases still needs more intensive experimental investigations of the unsteady viscous flow phenomena, such as the dynamic stall at the retreating side of the rotor and the complex mechanism of the stall in the vicinity of the blade tip. Overall flow field measurements on pitching airfoils, pitching finite blade models and on rotating blades in hover chambers and wind tunnels have been successfully performed at different places.

In this section we focus on measurements, which have been obtained for a steady incidence angle of 11.5°, since the flow phenomena involved are best understood and documented. This incidence angle corresponds to the point where maximum lift is obtained, shortly below the incidence angle where massive flow separation occurs. The flow around the OA209 profile for this range of Reynolds number, span wise location and incidence angle is determined by the transition of the boundary layer and the flow separation on the suction side which results in the generation of vorticity dominating the wake flow and the performance of the wing. This holds in a similar way for finite wings and 2D-airfoil profiles. For the present case of moderate Reynolds numbers and high incidence angles, laminar flow separation occurs shortly behind the leading edge and transition to turbulent flow conditions occurs immediately after separation. The resulting turbulence intensity forces a reattachment of the flow within a short distance, resulting in a significantly increased maximum lift with respect to the low Reynolds number cases. The separation together with the re-attachment forms a laminar separation bubble containing a recirculation region, which has only a few millimeter extension in chord wise direction (see figure 9.90). The turbulent boundary layer behind the bub-

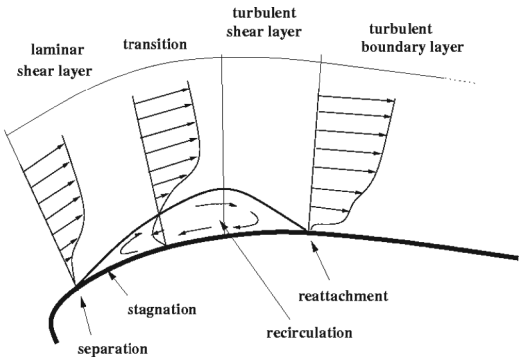

Fig. 9.90. Sketch of the separation bubble.

ble allows the flow to stay attached even at relatively high adverse pressure gradients.

Detailed investigations of the turbulence intensity, the size and the temporal development of the flow structure at the leading edge are required in order to validate CFD-codes which are under development for a more accurate prediction of the dynamic stall cases. Therefore, stereoscopic PIV and pressure measurements have been performed to quantize the overall flow features close to the tip of a rotor blade, both in steady cases and during pitching motion. Two-components PIV measurements with an observation field size of 1 mm and 50 μm resolution, have been performed further inboard in order to resolve the relevant flow features in the phase shortly before the stall onset in steady and unsteady cases. The results of the steady case have been compared with ELDV (Embedded Laser Doppler Velocimetry see [431]) and CFD data.

9.19.2 The Test Setup

The laser system used had 2×200 mJ pulse energy at 532 nm and was equipped with conventional light sheet optics. The cameras had a resolution of 1280×1024 pixel.

The setup used for the PIV measurements with a very high resolution is similar to the one described in [432], but has been used under relatively rough conditions in a wind tunnel. The microscope lens used for the test was a mirror objective lens QM100 of Questar Corporation. It is optimized for working distances G, ranging from $G = 150$ mm to $G = 380$ mm. It has an aperture angle of $\omega = arctg(D/2G)$ with D being the aperture diameter. The numerical aperture for the working distance of $G = 355$ mm, which has been chosen for the experiment, is $A = n \cdot sin\,\omega = 0.083$ with n being the refractive index of air. The F-number was $f_{\#} = 1/2A = 6$ and the magnification $M = 4.86$ resulting in a calibration factor of 754 pixel/mm. The diffraction limited minimum image diameter was $d_{diff} = 2.44\ f_{\#}(M + 1) = 45.6\,\mu$m and the estimated depth of focus $\delta Z = 2f_{\#}d_{diff}(M + 1)/M^2 = 136\,\mu$m. The light

sheet thickness was also 400 μm. Particle image diameters observed were between 50 and 130 μm (8–20 pixel) which is similar to observations made in [283, 284]. The development of the boundary layer, the reverse flow region and the shear layer towards the outer flow can clearly be seen in the results presented below.

The experiments have been performed in the S2 Luminy wind tunnel of the Laboratoire d'Aérodynamique et de Biomécanique du Movement LABM of the French research center CNRS at the University of Marseille. The PIV measurements were performed close to the leading edge of an OA209 blade tip model, in a plane orthogonal to the span in a distance of approximately 200 mm.

The majority of the μ-PIV measurement has been made at a steady incidence angle of 11.5° and has been compared with CFD and ELDV results at the same condition.

9.19.3 Results and Discussion

The image quality obtained with the mirror telescope objective, allows for the analysis of the unsteady flow features at a spatial resolution of $\simeq 50\,\mu$m. The number of outliers is of the order of 5%. The relative accuracy, as compared to conventional PIV recordings, is slightly lower due to the fact that the particle images are approximately five times larger. However, the uncertainty due to noise is assumed to be in the order of 0.1 m/s and the wall distance of each measurement location can be determined very precisely, since the surface is visible in each recording. Therefore, the development of the boundary layer, the reverse flow region and the shear layer towards the outer flow can clearly be seen in the result figure 9.91.

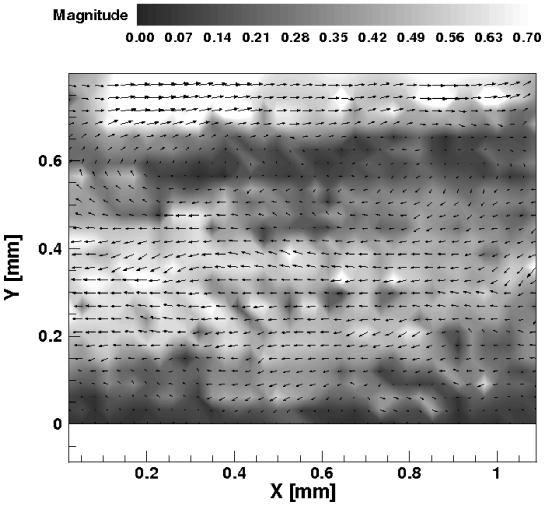

Fig. 9.91. PIV results obtained with a mirror telescope objective at $\alpha = 11.55°$, steady case. The magnitude of the velocity has been plotted by gray levels. The coordinates x and y are given in millimeters. The origin is placed on the model surface (y), 5% chord length behind the leading edge (x).

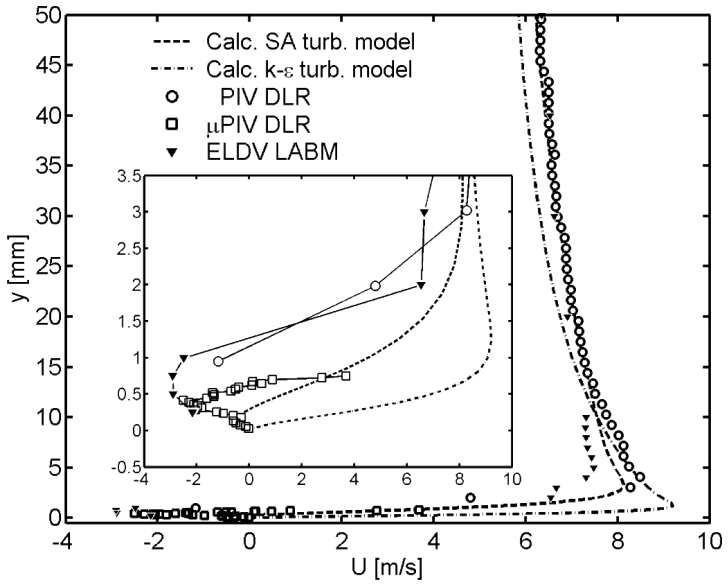

Fig. 9.92. CFD, ELDV and PIV results of the laminar separation bubble at $\alpha = 11.5°$ and $x/c = 0.05$; steady case.

Figure 9.92 depicts tangential velocity profiles through the laminar separation bubble obtained by CFD with SA- and SST turbulence models and by ELDV, PIV and μPIV. It can be seen that the agreement of most of the different methods in the outer regions (20 mm and above) is relatively high ($\sim$98%) with respect to the free stream velocity). However, the more detailed presentation in figure 9.92 shows that the differences between the different experimental results as well as of the different CFD results becomes evident. The reason for the differences of the PIV and the μ-PIV results can easily be explained by the weak spatial resolution of the recordings made with the 100 mm-lens. The differences between the ELDV measurements and the μ-PIV measurements are more significant and differ not as much in the measured flow velocity, but in the size of the separation bubble in wall normal direction. One reason for this might be a small disagreement of the incidence angle adjustment of both tests. However, the conclusion, the conclusion which turbulence model resolves the flow field in the separation bubble best, can easily be drawn in favor for the SA-turbulence model.

9.19.4 Conclusions

Discrepancies concerning the size of the separation bubble on a helicopter blade profile have been observed as well as an acceptable agreement of the velocity magnitudes found by the different measurements. The present results can be considered to be a good data basis for the validation of numerical

codes. However, the finely structured vortices observed at high incidences and their complex evolution during some phases of the pitching motion is not yet sufficiently predicted by two-dimensional computations. It has been demonstrated that instantaneous velocity fields determined by PIV at high spatial resolutions can be used to choose turbulence models and numerical damping coefficients. The strength, scale, and distribution of the laminar separation bubble - measured for the first time with such a high resolution in a wind tunnel experiment - are essential for the validation of numerical simulation techniques.